Heliyon 10 (2024) e28402

Contents lists available at ScienceDirect

Heliyon

journal homepage: www.cell.com/heliyon

Research article

# Renewing the potential of rice crop residues as value-added products in the cosmetics industry

Paola Vargas-Escobar [a,*], Oscar Flórez-Acosta [a], Ligia Luz Corrales-García [b]

[a] Department of Pharmacy, Faculty of Pharmaceutical and Food Sciences, University of Antioquia, Calle 67 N° 53 - 108, Medellín, Colombia
[b] Department of Food, Faculty of Pharmaceutical and Food Sciences, University of Antioquia, Calle 67 N° 53 – 108, Medellín, Colombia

ARTICLE INFO

*Keywords:*
Straw
Husk
Proteins
Carbohydrates

ABSTRACT

Purpose of this study is to explore the extraction of potentially valuable cosmetic ingredients from rice crop residues, aiming to mitigate their environmental impact.
*Methods:* We employed AOAC methods to analyze the fat, protein, ash, fiber, soluble, and insoluble carbohydrate content in these residues. To identify sugars rich in galactose and acidic sugars, a total soluble carbohydrate extraction was performed. Cellulose, as part of the insoluble carbohydrates, was isolated through alkaline and acid hydrolysis, while sodium silicate was derived from the ash. Characterization of insoluble cellulose and silicate involved techniques like FTIR, DSC, PXRD, microphotography, porosity assessments, and water absorption studies. For proteins, alkaline solubilization and precipitation at the isoelectric point were utilized, with quantification via BCA and amino acid profiling through gas chromatography. Evaluation of radical scavenging capacity using DPPH led to the calculation of apparent molecular weight via SDS-PAGE.
*Results:* The results revealed low levels of gum, mucilage, and pectin in both residues, contrasting with a high concentration of insoluble polysaccharides. Among these, Iβ cellulose displayed potential attributes for cosmetic applications due to its oil and water adsorption characteristics. However, silicates obtained from the ashes did not exhibit direct use potential. In terms of protein extraction, we observed antioxidant properties, with enhanced performance through enzymatic hydrolysis, achieving a hydrolysis degree of 30.41% and a DPPH radical absorption rate exceeding 70%.
*Conclusion:* Rice residues, particularly husk and straw, shown valuable substances suitable for potential cosmetic applications, encompassing cellulose, hydrolyzed proteins, and ash as a silicate precursor.

## 1. Introduction

Rice is one of the most widely consumed foods in the world. Annual production exceeds 514 million tons grown on five continents [1]. It is estimated that the annual demand for rice will be maintained due to demographic and economic growth; however, as with other agri-food products, an increase in its production generates a rise in the number of by-products derived from it, which include broken rice, rice flour, crushed rice, bran or husk, and the plant as yerba or straw, obtained after cutting. For example, for every part of grain processed, there are 0.2 parts of husk and 1–1.4 parts of straw [2], which, if not properly used, produces a large amount of

* Corresponding author.
*E-mail address:* paola.vargase@udea.edu.co (P. Vargas-Escobar).

https://doi.org/10.1016/j.heliyon.2024.e28402
Received 22 October 2023; Received in revised form 16 March 2024; Accepted 18 March 2024
Available online 27 March 2024

pollution spilled into the environment from these agricultural wastes. Nowadays, consumers are more aware of the use of natural resources and the management of the waste they produce, so there is an opportunity to convert waste and by-products from agricultural or industrial processes into raw materials or inputs for other processes, generating benefits and reducing of the environmental impact caused by the inadequate management, this process is known as supra recycling, also called "upcycling". In the cosmetic world it is an innovative practice that goes beyond sustainability and began with the use of coffee grounds or fruit peels that had been discarded, turning them into ingredients for cutting-edge natural exfoliants. That is, instead of simply recycling materials, upcycling involves creating new ingredients from waste, which reduces the amount of waste and, in turn, helps protect the environment. Another benefit of upcycling is that it can help companies reduce not only their production costs, but also their carbon footprint.

Some reports have long documented the properties of rice endosperm for dermal use and as a cosmetic ingredient [3]. For example, baths with rice water have been used, especially in Asia, where a starch gel, prepared from washed and boiled grains, is applied to the skin and scalp [4], but there are few reports on the use of its residues in cosmetics.

The most representative residues of the rice harvest and production are straw and husk, both represent more than 20% of global production, straw and husk contain 32–38% cellulose, respectively, which gives them a high potential as a source for the production of cellulose at low cost, allowing us to maximize the potential for using this waste and minimize the environmental impacts generated by burning and water contamination.

Carbohydrates, a large group of molecules found in rice plants with a typical structure of polyhydroxyaldehydes or polyhydroxyketones, have potential activity as pharmaceutical and cosmetic excipients; for example, cellulose and its derivatives are carbohydrates obtained from renewable resources that have been approved as cosmetic ingredients by the Personal Care Products Council (PCPC) and listed in the Cosmetic Ingredients Database (CosIng), as abrasives, absorbents, anti-caking agents, fillers, emulsion stabilizers, exfoliants, opacifiers, and flow and surface modifiers [5–10]. Cellulose is also used as an emulsion stabilizer (with low allergenic potential), skin moisturizer, lipid absorber, skin permeability enhancer for some active and functional ingredients [10], substitute for exfoliants in toothpaste or soaps (avoiding microplastic pollution).

The second main compound in rice plant residues is ash, which has great potential in the cosmetics industry due to its high silicate content but is more widely used in other industries [11–13]. Silicates are a wide series of related compounds whose properties vary depending on the characteristics of the method and the components used to obtain their salts [14]. Structurally, in the solid state, sodium silicates can occur in different forms, established in phases or polymeric layers of complex polymorphism from sodium cations, of which the most common phases are δ, α, and β [15]. Sodium silicates are salts with a silicate as a counterion and the general chemical formula $(Na_2O)_xSiO_2$. The proportions of sodium oxide ($Na_2O$) and silicon oxide ($SiO_2$) can produce different compounds with different physical and chemical properties. $Na_2SiO_3$ is called sodium metasilicate or water glass, the most abundant and widely used sodium silicate [16].

Studies showed that the appropriate addition of silicates to some cosmetic products could increase collagen and elastin production for skin firming, and their high buffering capacity helps to reduce potential irritation problems; they help as moisturizers, especially in the form of nanoparticles [17]. Silicates can also be used in the cosmetics and cleaning industry as excipients when they are converted into silica, which in turn are used to obtain Pickering oil/water (o/w) emulsions due to their gelling power, or as bleaching agents, or soaps and detergents, or as adjuvants to facilitate the absorption of other components [18].

On the other hand, although the protein content in both wastes is not as representative as insoluble carbohydrates and ashes, the recovery of the protein allows to obtain ingredients with high added value, with differentiated functions and potential as active ingredients than can be used in applications for skin and body care [19]. The potential benefit of the protein material is given by some low molecular weight peptides (protein hydrolysates) that could prevent oxidation reactions by acting as reducing agents and protecting cells from oxidation, either when incorporated into the diet or applied in formulations. Indeed, topical use of peptides avoids skin damage caused by ultraviolet radiation and is also used against skin erythema [20]. However, there are few reports on extracting peptides or proteins with antioxidant properties from rice straws and husks.

Antioxidants are important in cosmetics because they help combat skin aging. Antioxidants neutralize free radicals, which are unstable molecules that steal electrons from healthy cells to stabilize themselves and weaken healthy cells in the process, causing oxidative stress and premature aging [21]. Some research has concluded that antioxidants are more effective than sunscreens in protecting the skin from cancer because they are capable of creating a barrier capable of protecting it from ultraviolet rays and infrared radiation [22,23].

Finally, bran is the main source of lipids in the rice plant (15%–25%); the gamma-oryzanol is a remarkable compound due to its therapeutic properties such as hypolipidemic, antidiabetic, anti-inflammatory, and anticancer [24,25]. Rice bran wax is probably the most widely used ingredient in cosmetics; however, the lipids found in the rice grain are a minor component when compared to carbohydrates, ash, and proteins, and their presence in the other parts of the plant is practically negligible [26].

This research aims to find interesting bioactive raw materials from rice crop residues as an alternative for the cosmetic industry. Rice by-products are a source of diverse macromolecules that can be used as ingredients of natural origin with different bioactivities and applications. The extraction of these undervalued residues would allow the commercial use of the components obtained with added value, promoting the use of the rice waste and helping to reduce environmental pollution.

## 2. Materials and methods

### 2.1. Materials

All reagents used were analytical grade. Acetic Acid, Sodium Acetate Trihydrate, Hydrochloric Acid, Sulfuric Acid, Ammonia,

Copper Sulfate, Acetone, (MERCK, US). Ethanol, Methanol, Sodium Hydroxide, Hexane, and Blue Comassie G (Honeywell, Charlotte, North Carolina, US). Sodium Dodecyl Sulfate, DPPH (2,2-difenil-1-picrilhidracilo), BCA (Bicinchoninic Acid Disodium Salt) (Poner la marca de estos reactivos anteriores y país). Flavorzyme® (protease from Aspergillus oryzae with activity 500 U/g), Alcalase® (protease from Bacillus licheniformis; specific activity 2.4 AU/g (Sigma Aldrich, US). Phosphoric Acid and EDTA (J.T BAKER, Pennsylvania, US). SeeBlue Plus Prestained Standard (BioRad, US).

### 2.2. Methods

#### 2.2.1. Material obtention and pre-treatment

Straw and paddy-type rice husks were cut and collected in Campo Amor, Huila, Colombia. The material was dried in an air convection oven at 45 °C for 24 h and milled to a fine and homogeneous powder using a blade mill; after this process, the residues were defatted with acetone (3 Acetone:1 Residue), then the acetone was evaporated in an air convention stove.

#### 2.2.2. Composition of waste

Dry and defatted residues were chemically characterized to determine the content of fats, proteins, ashes, and fiber [27,28].

#### 2.2.3. Soluble carbohydrates

*2.2.3.1. Total carbohydrate extract (TCE).* Pre-treated plant material (straw and husk) was enzymatically digested with papain (10% w/w regard to dry material) in a buffer solution (0.1 M sodium acetate, 0.05 M EDTA, and 0.050 M cysteine, pH 5.5) at 50 °C for 2 h. The enzyme was inactivated by increasing the pH (to 10). The samples were centrifuged in three consecutives repetitions (Eppendorf 5810R) at 3538 *g* for 20 min. Carbohydrates in the obtained supernatants were precipitated by adding ethanol in a ratio of 3:1 (Ethanol: sample) (24 h, 0 °C); the precipitation process was repeated until no precipitate was obtained. Finally, the polysaccharide extract was washed in a 75% ethanolic solution, dried, and weighed.

*2.2.3.2. Total sugars.* The method proposed by Ref. [29] on straw and husk residues was used. Briefly, 3 mL of concentrated sulfuric acid were added to 1 mL sample of TCE (reconstituted in water (10 mg/ml), mixed, and allowed to cool in an ice bath; then, the absorbance was measured at 315 nm in a spectrophotometer (Genesys 10S UV-VIS Thermo Scientific, EU.). A glucose calibration curve (0.1 mg/mL and 0.0125 mg/mL) was used to calculate the concentration of the samples.

*2.2.3.3. Galactose-rich sugars (mucic acid test).* 1 mL of a sample was mixed with 1 mL of concentrated nitric acid and heated (80 °C) in a water bath for 90 min 5 mL of Milli-Q® IQ 7003 water (Merck) was added to each tube and allowed to stand for one week. The presence or absence of a white precipitate corresponds to mucic acid crystals. The assay was also performed with 10% w/v solutions of galactose and glucose as positive and negative controls, respectively.

*2.2.3.4. Acid sugars (carbazole test).* We followed the method proposed [30], where 5 mL of sodium tetraborate solution in $H_2SO_4$ were added to 1 mL of the sample. The mixture was heated in a boiling water bath for 10 min; then, 0.2 mL of carbazole were added while stirring and left in the bath for another 5 min. After cooling, the absorbance was measured at 530 nm. The concentration was calculated from a standard curve (4–40 μg/mL galacturonic acid).

#### 2.2.4. Cellulose crude extraction

The method proposed by Ref. [6] was used based on acid and alkaline treatments to obtain cellulose (8). The dry and ground samples were mixed in a ratio of 1:10 with a 5% NaOH solution for 3 h with constant heating at 74 °C. When the dispersion reached room temperature, the material was washed with distilled water to neutral pH. The resulting product was mixed with an excess of 5% NaClO for 24 h. Washing and filtering cycles were performed until a pH between 5 and 7; the resulting solid was subjected to hydrolysis with an excess HCl 2 N at 80 °C for 1 h, then washed and filtered. As initially proposed, the alkaline treatment and bleaching was repeated, followed by washing and filtration to neutral pH. Finally, the obtained filtrate was dried and sieved.

#### 2.2.5. Cellulose characterization

*2.2.5.1. Microphotographs with optical light microscope (OLM).* Photographs were taken using an inverted fluorescence phase contrast microscope (IN300T-FL, Amscope, E.U.) coupled to a digital camera (MU1203-FL, Amscope. E.U.).

*2.2.5.2. Fourier transform infrared (FT-IR).* Infrared spectra were recorded between 650 and 4000 cm-1 (Spectrum 100 FT-IR PerkinElmer spectrometer, E.U.).

*2.2.5.3. Differential Scanning Calorimetry (DSC).* 5.0 mg of the cellulose sample were heated from 25 °C to 500 °C at a rate of 10 °C min-1, in a Differential Scanning Calorimetry (DSC) (Fox-200 Netszch, Germany), under nitrogen atmosphere, using aluminum crucibles.

*2.2.5.4. Powder X-ray diffraction (PXRD).* Polycrystalline samples of cellulose were analyzed in an X-ray diffractometer (Malvern-PANalytical, UK), using 2θ CuKα radiation and scanning from 10° to 80°. The crystallinity index (CrI) of the samples was calculated according to Equation 1

$$\mathrm{CrI} = \frac{\mathrm{I22} - \mathrm{I15}}{\mathrm{I22}} \quad \text{Equation 1}$$

where, I22 and I15 are the net intensities (I) of the signal of the peak at 22° and the peak at 15°, respectively.

*2.2.5.5. Porosity (ε).* Porosity was measured according to equation (2). True density ($\rho_{true}$) was calculated using a helium pycnometer (AccupycII 1340, Micromeritics, US) with approximately 2 g of each cellulose sample from husk and straw and three independent measurements.

Bulk density ($\rho_{bulk}$) was determined by weighing 20 g of each sample, and its volume was measured in a 100 mL graduated cylinder. The bulk density was calculated following Equation (2):

$$\varepsilon = 1 - \left(\frac{\rho_{bulk}}{\rho_{true}}\right) * 100\% \quad \text{Equation 2}$$

*2.2.5.6. Oil absorption capacity (OAC).* The OAC was calculated using Equation (3). One g of the first sample (Pi) was deposited in 10 mL of sunflower oil and stirred for 30 min; the mixture was then centrifuged at 1593 g; the supernatant was removed, and the sediment was weighed (Pf).

$$\mathrm{OAC} = \frac{\mathrm{Pf} - \mathrm{Pi}}{\mathrm{Pi}} \quad \text{Equation 3}$$

*2.2.5.7. Swelling degree (SD).* 1 g of each cellulose sample from husk and straw was placed in 10 ml of water at 37 °C. the increase in volume generated by the sample addition was measured initially (Vi) and after 72 h (Vf). SD was calculated according to equation (4):

$$SD = \frac{\mathrm{Vf} - \mathrm{Vi}}{\mathrm{Vi}} x\ 100\% \quad \text{Equation 4}$$

*2.2.6. Obtention of crude silicates*

Straw and rice husk samples were calcined in a muffle (Centricol Ltda, Colombia) at 500 °C for 4 h. Then, according to the method of Uda et al. in 2020, one part of the ash was mixed with 20 parts of NaOH 2.5 M and digested at 100 °C for 4 h with stirring. The mixture was filtered, dried to constant weight at 40 °C, and sieved through 200 mesh (ASTM E11-61, Tyler®, E.U.) to obtain a fine dark powder, a hydrated mixture of sodium silicates and metasilicates. Different purification and differentiation steps are required depending on the material. The yield of crude silicates was calculated according to Equation (5):

$$\%\ \text{Crude silicate yield} = (\text{weight sodium silicate}) / (\text{weight ash}) \times 100 \quad \text{Equation 5}$$

*2.2.7. Silicates characterization*

The silicates were evaluated by OLM microphotographs, FT-IR (Fourier transform infrared spectroscopy), and PXRD (Powder X-ray diffraction), using the same method as the cellulose; additionally, the following tests were performed.

*2.2.7.1. Determination of the buffering capacity (BC).* One g of a silicate sample was placed in 50 ml of miliQ water pH 7 (Thermo Scientific, US); after 3 min, the pH was recorded and then titrated with HCl (0.1 N) to pH 4. BC is calculated by dividing the milli-equivalents of HCl by the total change in pH units (from initial pH to pH 4) [31].

To consider a relatively high buffering capacity, a 0.5% aqueous solution of the silicate samples should have a pH of around 12.5.

*2.2.7.2. Thermogravimetric analysis (TGA)/Differential Scanning Calorimetry (DSC).* The TGA/DSC analysis was performed using the Discovery STD 650 instrument (TA instruments US). 5.0 mg of sample were heated from 25 °C to 900 °C at 10 °C $\mathrm{min}^{-1}$ under N atmosphere, using Al crucibles.

*2.2.8. Protein extraction*

A defatted sample (Husk and straw) was mixed with water in 1:5 ratio, and the pH was adjusted to 10 with NaOH 1 N and 1 mmol of EDTA as a chelating agent to avoid proteolysis. The mixture was incubated for. 3 h at 40 °C with continuous agitation. Then, it was centrifuged (29,906 g for 20 min), and the supernatant was adjusted to its isoelectric point (IEP) (Measuring the pH until zeta potential is zero) with HCl 1 N; the mixture was cooled at 5 °C and centrifuged at 1593 g, 10 °C for 20 min. The protein was dried, and finally, the yield was found using Equation (6):

$$\%\ \text{Protein yield} = \frac{\text{initial residue weight} - \text{proteic extract weight}}{\text{initial residue weight}} \quad \text{Equation 6}$$

### 2.2.9. Protein characterization

*2.2.9.1. Protein quantification.* The amount of protein was quantified by bicinchoninic acid (BCA) (Sigma Aldrich, US) [32] and measuring absorbance at 562 nm. A calibration curve was constructed with bovine serum albumin (BSA) (Sigma Aldrich, US) as standard from 0.1 to 10 mg/mL.

*2.2.9.2. Determination of apparent molecular weight.* SDS-PAGE determined the apparent molecular weight profile of the straw and husk samples in a Mini-PROTEAN Tetra vertical electrophoresis cell chamber (Biorad, US) at a constant voltage of 120 V. Samples were mixed with sample buffer to ensure 50 μg of protein in each well. Standard Precision Plus Protein Dual Xtra was used as a molecular weight marker (Biorad, US))

The gel was stained with 0.1% (w/v) Coomassie Brilliant Blue R250 for 1 h and destained with a mixture of 5% (v/v) methanol, 7.5% (v/v) acetic acid, and 87.5% water to visualize protein bands. Gels were preserved in 7% acetic acid and photographed for later analysis.

*2.2.9.3. Isoelectric point measurement (IP).* Solutions with a pH between 2.0 and 12.0 were prepared, adding HCl 0.1 M and NaOH 0.1 M, as appropriate 0.1 g of the protein sample was added to each solution and stirred for 2 h to stabilize the pH; then, the zeta potential was measured in the zetameter (Malvern Instruments, UK). The isoelectric point corresponds to the pH value at which the zeta potential is zero. The IP is found by fitting the curve to a model and interpolating the pH value at which the potential is zero.

*2.2.9.4. Amino acidic profile.* Samples and amino acid standards were injected on an Agilent 7890 Gas Chromatography (GC) system (Wilmington, DE, US) equipped with a 5975C mass spectrometer (MS) detector (Santa Clara, US and an HP-5ms column (30 m × 0.25 mm x 0.25 μm) (Santa Clara, US). 10 mg of each sample were dissolved in distilled water; the proteins were precipitated with acetone, resuspended in alkaline water (pH 10.0), and centrifuged at 29,906 g for 20 min. Aliquots of the supernatant were dried and derivatized with pyridine and N, O-Bis Trifluoroacetamide (BSTFA). Finally, the samples were heated (70 °C) for 3 h and injected into the gas chromatograph. Identification was made by comparing the retention time and fragmentation pattern of the amino acids present in the samples with reference standards.

*2.2.9.5. Antioxidant capacity analysis.* The DPPH free radical method was used to evaluate the antioxidant capacity of proteins [33], measuring the absorbance decay of the samples at 517 nm, after 30 min (Ai), and after incubation in the dark (Af). The results are reported as % radical uptake using Equation (7):

$$\%\ \mathrm{DPPH} = \frac{\mathrm{Ai} - \mathrm{Af}}{\mathrm{Ai}}\ \mathrm{x100} \qquad \text{Equation 7}$$

Free radical scavenging results are also expressed in TEAC (Trolox Equivalent Antioxidant Capacity), using a calibration curve at concentrations from 0.05 to 0.8 mM of Trolox (water-soluble analog of vitamin E). The values were calculated with Equation (8):

$$\mathrm{TEAC} = \frac{\mathrm{M\ x\ DF\ x\ V}}{\mathrm{w}}\ x\ 100 \qquad \text{Equation 8}$$

where M is the molar concentration obtained from the calibration curve; DF is the dilution factor with which the sample was prepared; V is the volume in liters at which the sample was initially prepared; and W is the weight in grams that was originally taken from the sample.

### 2.2.10. Enzymatic hydrolysis

Preliminary studies were conducted to find the best conditions for obtaining a protein hydrolysate with antioxidant properties using the commercial enzyme Alcalase® (Bacillus licheniformis protease; specific activity of 2.4 AU/g, Sigma Aldrich, US). Enzyme activity was measured by the free tyrosine release assay, following the universal protease activity assay using casein as substrate [34].

Briefly, 20 mg/ml of the protein concentrate was hydrolyzed using an enzyme/substrate ratio of 1:10 (v/v) at pH 10 and 50 °C. The hydrolysis was conducted in a beaker placed in a water bath (80 °C) at a controlled temperature between 80° and 90 °C. During the reaction, the water bath and the mixture were agitated to keep a uniform temperature throughout the system, and the mixture was kept at a constant pH by titration with 1 N NaOH. The total hydrolysis time ranged from 2.5 to 75 min. Upon completion of hydrolysis, the enzyme was inactivated by heating the hydrolysate mixture to 80 °C for 15 min; then cooling to room temperature, neutralizing, and centrifuging at 25,482 g for 10 min. The hydrolysate supernatants were stored for further analysis. The kinetics were plotted as a function of time, with the degree of hydrolysis (DH) measured as the response variable.

*2.2.10.1. Degree of hydrolysis (DH).* DH is defined as the proportion of peptide bonds cleaved in a protein hydrolysate, determined using the pH-stat method [35] and based on the amount of NaOH consumed to maintain a constant pH during hydrolysis. The DH value is expressed by Equation (9):

$$\mathrm{DH} = \frac{Bx\,N}{M}\ x\ \frac{1}{h_{tot}}\ x\ \frac{1}{\alpha} \qquad \text{Equation 9}$$

where B is the amount of NaOH (mL); N is the normality of NaOH; M is the initial mass (g) of the hydrolyzed protein; $h_{tot}$ is the theoretical total number of peptide bonds in the protein substrate and, in this case, it is taken as a reference value of 7.40 mmol/g; α represents the average degree of dissociation of the a-$NH_2$ groups in the protein substrate and is expressed in Equation (10):

$$\alpha = \frac{10^{pH-pK}}{1+10^{pH-PK}} \quad \text{Equation 10}$$

where pH and pK are the values at which proteolysis was conducted (9.465 is the average pK of the amino acids at 25 °C.

*2.2.10.2. Antioxidant capacity analysis.* The previously described DPPH free radical method was used to evaluate the antioxidant capacity of hydrolysates [33].

## 3. Results and discussion

### 3.1. Sample material composition

We used the AOAC methods to find protein, fat, ash, and moisture. The carbohydrate content was calculated by the difference from the dry material. Our results are consistent with other previously reported, with a high carbohydrate content, low protein levels, and a low amount of crude fat (Table 1) [36].

Carbohydrates are mostly insoluble fiber, such as lignocellulose, a potential source for low-cost cellulose production [9] In addition to insoluble fiber, there are also water-soluble polysaccharides of cosmetic or pharmaceutical interest, such as pectins, gums, and mucilages [37].

Ashes, from the rice husk and straw incineration, have silicates, a promising source that can provide competitive value to this crop in many industries, including cosmetics. Additionally, the treatment of ashes, due to their relatively high silica content and abrasive properties, contributes to reducing the environmental impact caused by the disposal of this waste [38].

The third most abundant component in both residues was protein, with a high potential in developing antioxidants for the food and pharmaceutical industries [39]. Antioxidant peptides can be obtained by hydrolyzing proteins with endogenous or exogenous enzymes or by microbial fermentation, with enzymatic hydrolysis being the most widely used in the food and cosmetic sectors [39–43].

### 3.2. Soluble carbohydrates

#### 3.2.1. Total sugars, galactose-rich sugars and acid sugars

The soluble carbohydrate analysis (Table 2) suggests that both straw and husk are not a source of gums, mucilages, or pectins, which is consistent with previous reports for these residues; e.g., according to Banerjee et al., 2009, the rice husk without any pre-treatment did not contain free glucose or xylose, and after hot air oxidation processes, the increase in free monomers in the liquid fraction was low [44]. Few reports are available about other components, such as pectins. An analysis conducted by Ref. [45] found that the amount of pectins after acid treatment varied between 1.2 and 3.6% for rice straw.

In rice straw, we found monomers such as glucose, xylose, and arabinose, which are the major components of cellulose and hemicelluloses quantified after successive acid hydrolysis processes (Kim et al., 2010). Other glucose or fructose compounds have been reported in the stems during plant growth, including starch, (1 → 3) (1 → 4) glucan, sucrose, free glucose, and free fructose; however, direct sun drying reduces the amount of these sugars, which explains the absence of free soluble carbohydrates in our samples, dried directly in the field [46].

According to the composition of soluble carbohydrates, cellulose could be the material to be extracted from the lignocellulosic residues of the rice.

### 3.3. Obtaining crude cellulose

A fine white powder was obtained for the straw and slightly yellow one for the husk, with a yield greater than 30% in both samples (Table 3).

The cellulose of the straw has a whitish appearance, mostly fibrous, organized in regular lines (Fig. 1b); while the cellulose of the husk has a slightly pale-yellow color, and the structure corresponds to a non-symmetrically intertwined fiber (Fig. 1a).

**Table 1**
Percentage composition of rice crop residues.

| | Straw | Husk |
|---|---|---|
| Dry material (%) | 89.2 ± 1.9 | 90.7 ± 0.06 |
| Proteins (%) | 1.9 ± 0.33 | 4.7 ± 0.98 |
| Crude fat (%) | 0.2 ± 0.00 | 0.4 ± 0.01 |
| Ashes (%) | 16.5 ± 0.06 | 20.8 ± 0.10 |
| Carbohydrates (%) | 70.50 | 64.60 |

**Table 2**
Result analysis of soluble carbohydrates.

| | Husk | Straw |
|---|---|---|
| **Total soluble sugars** | 8.92 mg/ml **(0.11%)** | 1.89 mg/ml **(0.23%)** |
| **Galactose-rich sugars (Mucilages)** | Absence | Absence |
| **Acid sugars (Gums and pectins)** | 0.47 mg/ml **(0.0058%)** | 0.4292 mg/ml **(0.0053%)** |

**Table 3**
Waste cellulosic material.

| | Husk | Straw |
|---|---|---|
| **Cellulose** | 32.925% | 30.587% |

### 3.3.1. Cellulose characterization

*3.3.1.1. FT-IR of cellulose.* Both celluloses showed similar bands in the infrared spectra (Fig. 2), such as the absorption band close to 2900 $cm^{-1}$, which is related to the stretching and bending of the CH and $CH_2$ bonds, and the 1316 $cm^{-1}$ with the O–H bending, characteristic of the D-glucose units linked by β (1 → 4) glycosidic linkages. The absence of bands at 1735 $cm^{-1}$ and 1253 $cm^{-1}$ corresponding to vibrations of the carbonyl group suggested the lack of ether-type bonds and, therefore, no lignin in the samples.

*3.3.1.2. Cellulose DSC analysis.* The DSC thermogram of the celluloses was consistent with that reported by Ref. [47] (Fig. 3), where the amorphicity of both samples was observed, with exothermic signals in the range between 50 and 100 °C, corresponding to the loss of water. Broad peaks around 311 °C for the cellulose from the straw and 337 °C for the one from the husk were attributed to the decomposition of the cellulose due to the depolymerization reaction and the breaking of the glycosidic bonds that were assumed to be levoglucosan, accompanied by the decarboxylation of the compounds [48,49].

*3.3.1.3. Cellulose PXRD and crystallinity index calculation.* The diffractograms of the two samples were characteristic of Iβ cellulose, corresponding to the lattice planes ($I_{101}$) and ($I_{002}$), with intensities of the strong crystalline peaks at 15.8° and 22.6°, in addition to weak crystalline peaks with an intensity of 34.7° corresponding to plane 004 (Fig. 4) [50–52]. From these values, the crystallinity index was calculated, where the CrI of 46.26 % was for the straw residue and 52.20 % for the husk; they were values obtained from cellulose extraction without progressive treatments to eliminate amorphous materials [53]. Straw cellulose presented the lowest CrI and, therefore, higher amorphicity, as might be expected in cellulose from cell walls, such as cotton and wood [54]. However, the CrI

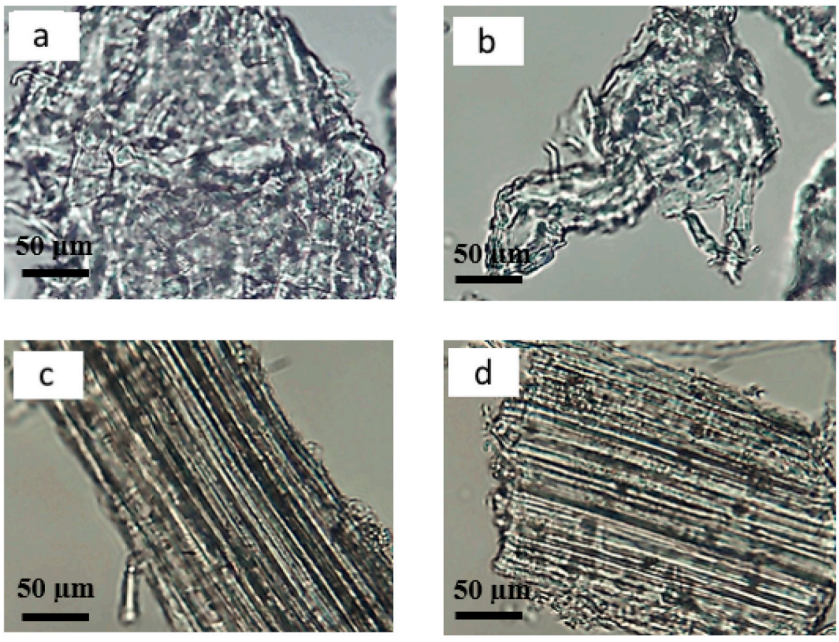


**Fig. 1.** OLM microphotographs (40X) of individual cellulose particles: a and b, cellulose obtained from the husk; c and d, cellulose obtained from straw.

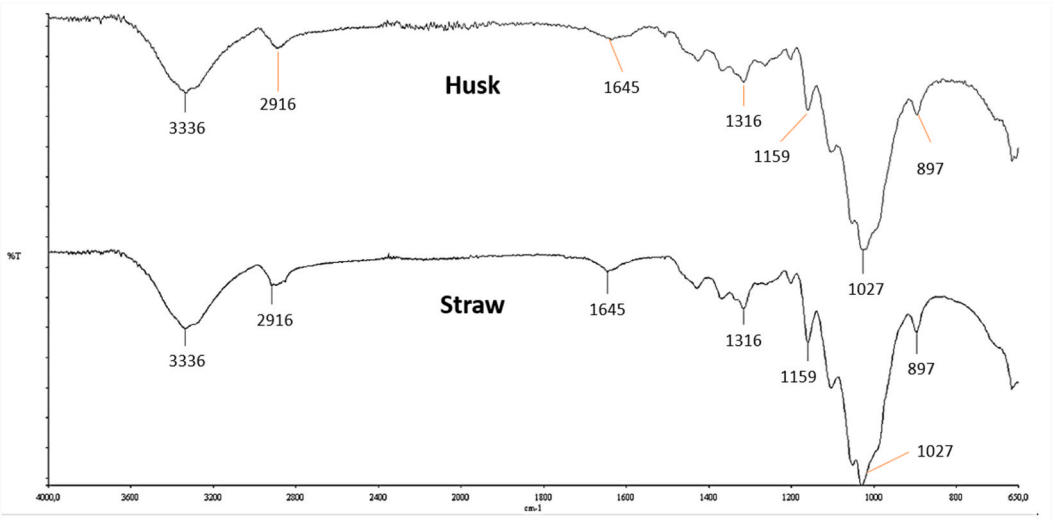


**Fig. 2.** Infrared Spectrum of cellulose crude extracted from rice residues.

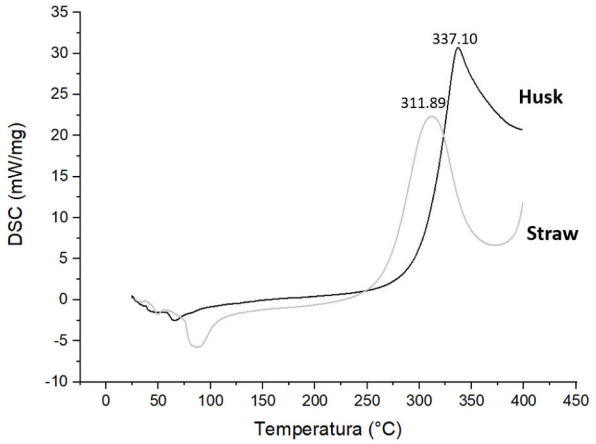


**Fig. 3.** DSC Thermograms of Cellulose crude extracted from rice waste.

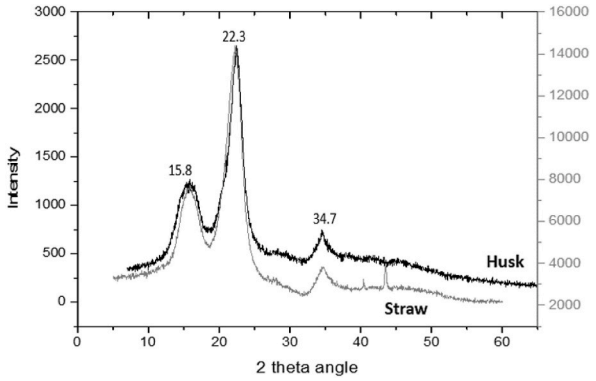


**Fig. 4.** Diffractogram of crude cellulose obtained from Husk and rice straw.

values can be influenced by the size of the crystals, which can overestimate the presence of amorphous material due to overlapping diffraction peaks near the $I_{101}$ plane area [54–56].

Both types of cellulose can be used as rheology modifiers for the cosmetic industry, and the degree of crystallinity, which is directly related to the values of Young's modulus and hardening, that is, the increase in viscosity, can be modified by the processes of refinement applied to them [57].

*3.3.1.4. Oil adsorption capacity of cellulose.* In the case of the cellulose derived from straw residues, the oil absorption was 16.0 %, and tha of the husk was 10.7 %, which indicates that they have significant potential in the cosmetic field, mainly in the category of makeup or decorative cosmetics, for its attributes to achieve mattifying effects or reduction of skin shine [58,59].

*3.3.1.5. Cellulose swelling degree (SD).* With the cellulose from these two residues, the SE of the straw cellulose stands out, with an absorption of 116.0 %, while that derived from the husk was 26.1 %, and although both could be used as absorbent materials, the cellulose derived from straw presented an extraordinary capacity for water absorption. This difference can be attributed to the intertwined cellulose fibers: in the straw with linear fibers, liquid can easily penetrate, separate, and lodge in the physically connected chains, while in the husk with interlocking and more united shell structures, the entry of liquid is more complex [60].

### *3.4. Silicates obtention*

A very high yield of raw sodium silicate was obtained from the ash in both samples, 88.2 % for straw residues and 88.9 % for husk residues, similar to previous reports by other authors [61–64]. These data show that rice husk is a residue that can be a major source of silicates.

#### *3.4.1. Sodium silicates crude characterization*

Crude functional compounds were obtained in this study; for example, silicates may be accompanied by inorganic compounds from the ash, such as $Na^{+}$, $K^{+}$, $Mg^{2+}$, and $Ca^{2+}$ cations [65,66].

#### *3.4.2. Silicates buffer capacity (BC)*

The sodium silicate of the rice straw had a BC of 70.2 mL and a pH of 10.8, while that of the rice husk was 55.3 mL and a pH of 11.08. These were the expected results for raw silicates and show the need to apply subsequent purification procedures if they are to be used as pH buffering agents in cosmetic products.

#### *3.4.3. Optical Light microscope (OLM) of sodium silicates*

Heterogeneous crystalline patterns in shape and size were found in both silicate samples (Fig. 5). The silicate particles obtained from straw are closer to the definition of blocky, while those obtained from husk have a flaky appearance. In addition, according to

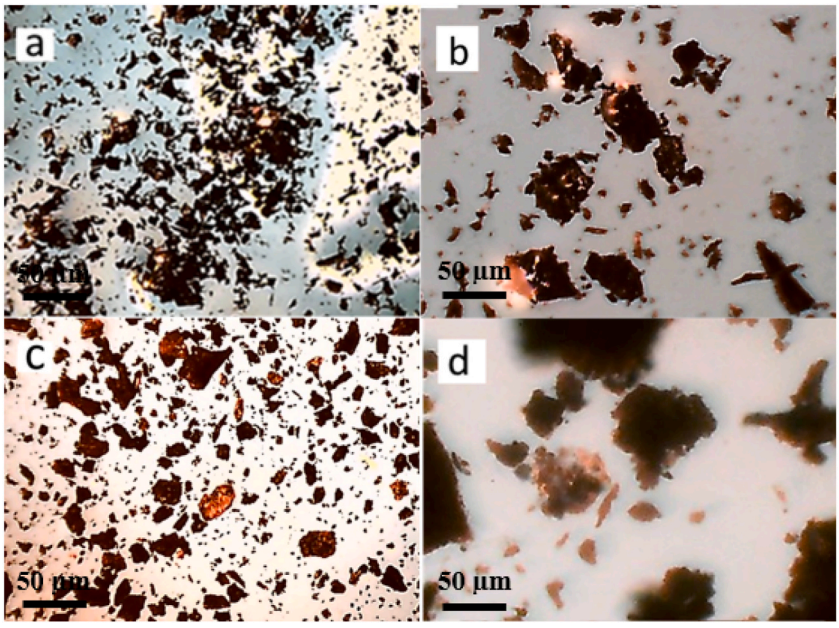


**Fig. 5.** OLM microphotographs showing the external appearance of the sodium silicate particles: **a.** 10X and **b.** 25X extracted from straw; **c.** 10X and **d.** 25X obtained from husk.

what was seen in the images of Fig. 5, the silicates obtained from the husk have a larger particle size than those derived from the straw.

### 3.4.4. FT-IR analysis of sodium silicates

The infrared spectrum of the two silicate samples showed similar signals (Fig. 6). The spectra showed predominantly the characteristic frequencies of the silicates, such as the representative Si–O–Si bands at 1060 cm $^{-1}$ (asymmetric stretching), which indicated the existence of cyclic siloxane tetramers, also associated with the vibratory effect, enhanced by another low-intensity peak at 880 $cm^{-1}$ (corresponding to the symmetrical stretching Si–O vibration).

A band at 1400 $cm^{-1}$ was also observed corresponding to $M^{+} - O$ (mostly Na–O), and a broader band around 2970 $cm^{-1}$ for O-species, possibly due to the transformation in the β-$Na_2Si_2O$ phase or to the presence of metasilicates because of high-intensity signals around 1400 $cm^{-1}$ and peaks at 1230 $cm^{-1}$ and low intensity at 880 $cm^{-1}$, which are events associated with a decrease in the $SiO_2$: $Na_2O$ molar ratio and an increase in free OH ions [67,68].

These results could be influenced by the presence of inorganic oxides M − O, which, although not measurable in the infrared, could affect the absorption of other species, for example, the narrowing of the O–H or H–O–H signals that should appear in the range of 3000–3500 $cm^{-1}$. Due to the high pH of the silicate solutions, the SiO(OH)− anions were more free, and the available OH functions decreased the width and intensity of the band, appearing at 2970 $cm^{-1}$; due to the O–H tension of NaOH and the absence of hydrogen bonding, a pronounced peak appeared at 3675 $cm^{-1}$.

Characterization of the solid state of silicates.

### 3.4.5. PXRD analysis of sodium silicates

The results showed differences in the internal structure of both samples (Fig. 7). The absence of broad peaks in the diffractograms confirmed an arrangement of silicates with incomplete amorphization, with little crystalline phase, represented by the content of the various $SiO_2$ polymorphs and the presence of the inorganic cationic oxides that accompanied the $SiO_2$ in the ash, such as the peaks at 25° and 27° ($K_2O$) and those at 18° and 38° (MgO), in addition to the metasilicates and the hydrated silicates [69–71] Likewise, due to the contribution of hydroxides, carbonates, and sulfates that could be formed with these cations, compositions that depend on the temperature and the acid-alkaline nature of the samples [72,73].

### 3.4.6. TGA/DSC analysis

Except for a common sharp peak in both samples that appears at 591 °C, which is attributed to the rapid volatilization of the gases trapped in the samples, the other signals differed for the two silicates (Figs. 8 and 9).

In the results of the thermal analysis of the silicates from the straw (Fig. 8) a first signal is observed as a sharp endothermic peak at 95 °C in the DSC and a mass loss that appears between 70 and 150 °C in the TGA; an event attributed to the first dehydration with loss of physiosorbed molecular water.

Also, from the DSC, two dominant exothermic signals appear (Fig. 8), possibly due to the thermal events of the main mineral oxides (M + O) remaining in the ash and the dehydrated sodium silicate [64,74]; a maximum peak appears at 340 °C, which is justified by a second mass loss observed in the TGA between 300 and 390 °C. This can be attributed to the dehydration of the interstitial water between the gel layers formed by $M^{+}$–S–H [75]. In some reports, the formation of amorphous phases of silicates is correlated with pH. The acid-neutralizing capacity of silicates is one of the key factors in forming these phases in the solid state; for example, that of magnesium, which, together with the degree of hydration of the samples, can cause the formation of gels, bubbles, or foams of $M^{+}$-S-H [76,77].

Another maximum exothermic peak at 417 °C is also observed in the DSC curve, with a mass loss in the temperature range of

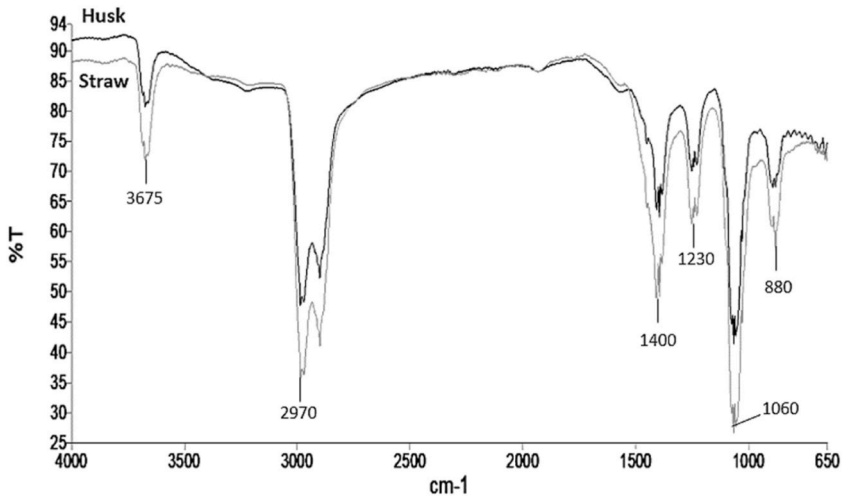


**Fig. 6.** Infrared Spectrum of sodium silicate crude extracted from rice residues.

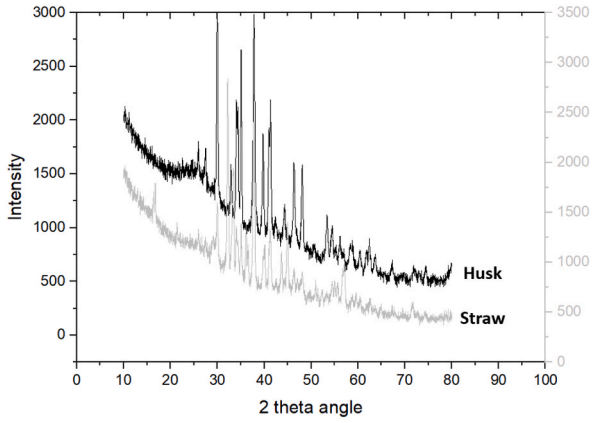


**Fig. 7.** Diffractogram of silicate crude obtained from Husk and rice straw.

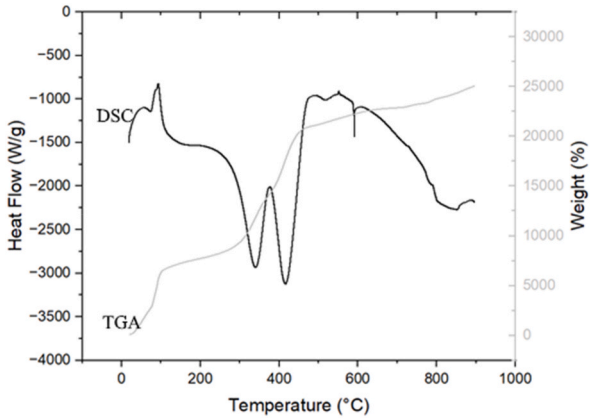


**Fig. 8.** TGA and DSC thermograms of sodium silicate of rice straw.

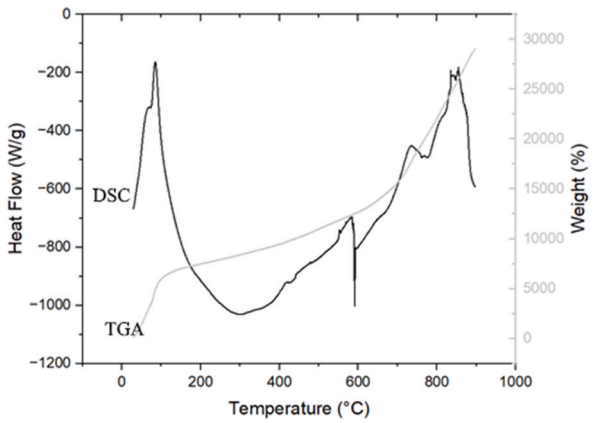


**Fig. 9.** TGA and DSC thermograms of sodium silicate of rice husk.

380–500 °C in the TGA curve. This thermal event has been previously reported as the dehydroxylation of the hydroxide groups of the minerals present and the silanol of the silicates, the elimination of some of the exchange anions, such as $CO_2$ and OH- of the calcium carbonates $M^{+}(OH)_n$, $M^{+}CO_3$ and from the $M^{+}$–S–H gel, and from the loss of residual water in the pores resulting from the reaction [78–81]. The last thermal event is an exothermic peak at about 850 °C in the DSC and a slight mass loss recorded between 720 and 890 °C, which was associated with the decomposition of $M^{+}$-S-H [82].

In the case of the thermal results of the silicates obtained from the husk ash (Fig. 9), peaks appeared with a specific trend above

200 °C in the DSC and a mass loss ranging from 100 to 650 °C in the TGA. These thermal events show structural changes within the solid, possibly because of pH, as previously expressed. As drying progresses, at around 200 °C, the material may swell and bubble, forming an impermeable foam layer outside the particles. This phenomenon of foam formation has been described as occurring in different stages and mainly affecting the largest particles, which could explain why silicates were found in the husk but not in the straw [83].

These solid state results showed that both types of silica obtained are amorphous and hydrated, which makes them suitable for cosmetic use and has no risk when inhaled, which could happen with the crystalline and anhydrous forms.

### 3.5. Protein extraction and quantification

Following the earlier described method with the dry and defatted sample for the protein extract of both residues, a performance close to 2 % was found. This performance is possibly due to the fact that alkaline extraction, although it allows greater protein recovery, presents as drawbacks the possible denaturation and hydrolysis of proteins, in addition to the extraction of non-protein components, which causes the obtaining of lower purity proteins, as was the case with the husk, which caused fewer proteins compared to those obtained. of straw (6.47 mg/mL vs 12.94 mg/mL). Alkaline extraction, due to the high pH, can also accelerate Maillard reactions with formation of melanoidin, giving rise to the dark brown products obtained [84].

#### 3.5.1. Protein characterization

*3.5.1.1. Isoelectric point measurement (IEP).* A common isoelectric point at pH of 1.75 was obtained for both samples, achieved by equalizing to zero the zeta potential in a plot of the charge of the protein solution as a function of pH. Adjusting the pH of the protein solution to this pH achieved greater precipitation, obtaining values of 1.87 % and 2.16 % for the husk and straw, respectively, while when the method previously reported by Naranjo and Suquilanda, where precipitation at pH 4.5 was proposed, the protein obtained was less than 1.5% [85].

*3.5.1.2. Determination of apparent molecular weight.* The electrophoretic profile showed a predominant band with a molecular weight of approximately 75 kDa, consistent with the processes for obtaining the protein concentrate, throughout the 2 independent extractions for each residue (Fig. 10). Additionally, it was possible to see that the concentration of the straw protein (12.94 mg/ml) is higher than that of the husk (6.47 mg/ml), confirming the results obtained in the quantification.

*3.5.1.3. Amino acids profile.* Leucine, arginine, and glutamine were found as common amino acids in both samples. The husk protein also had histidine, and the straw presented glycine and sulfur amino acids, methionine, and cysteine.

Both types of residues had a limited amino acid profile compared to the one reported by Khattab et al., 2013, for native forms, no processed straw, and husk; however, Kattab does not report cysteine as we do.

Regarding the amino acid profile, they showed a poor number of amino acids for the two residues (only 4 amino acids), compared to what was reported by Dario et al. in 2017, where almost all the amino acids were found in the sample, except for tryptophan. These divergences in the amino acid content can be explained by the difference in the varieties of rice evaluated, storage type, and drying of the samples [86].

*3.5.1.4. Antioxidant capacity analysis.* Both protein extracts presented a similar capacity to inhibit the free radical DPPH and TEAC (Table 4). The reports on DPPH in protein derivatives of straw and rice husks showed variations due to the different types of processes that were carried out on these residues [87–92].

The results showed that the protein extracts derived from the residues obtained had an antioxidant capacity comparable to standards, such as those used in the cosmetic and food industry, Butylated hydroxyanisole (BHA) with a DPPH of 22.16%, Butylhydroxytoluene (BHT) with a DPPH of 31.31 $\pm$ 2.4, Vitamin C with a DPPH of 28.8 $\pm$ 1.47, and Vitamin E with a DPPH of 25.1 $\pm$ 3.04; this activity was possibly due to the presence of highly reactive amino acids such as sulfur in the case of straw and histidine in the case of husk [93]. However, the antioxidant capacity not only depends on the amino acid composition present in the protein chain but is also influenced by their molecular weight; polypeptide chains sizes between 500 and 1800 Da t exhibit better capacity against large proteins and free amino acids, and in this case, proteins derived from these residues were around 125 kDa for both samples [39].

### 3.6. Degree of hydrolysis during the reaction

The enzymatic hydrolysis process was optimized only with the straw protein, since both protein samples had similar molecular weights and using only Alcalase®, because this enzyme provided a higher degree of hydrolysis and better antioxidant capacity compared to Flavorzyme ®.

The hydrolysis presented a kinetic behavior like that reported for other protein components (Fig. 11). Positive growth kinetics for % DH in the first hour of incubation, followed by decay at 75 min, possibly due to the reduction in the number of peptide bonds susceptible to hydrolysis, the inhibition of the enzyme by the products and/or substrates, or the inactivation of the enzyme [94–97].

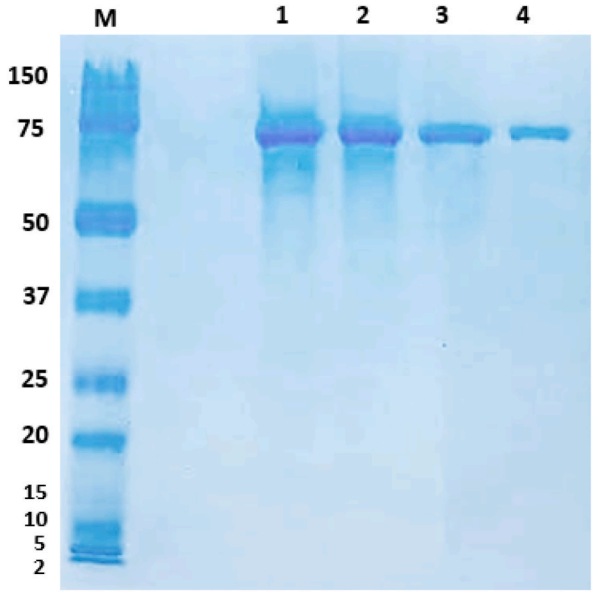


**Fig. 10.** Electrophoretic pattern proteins (SDS-PAGE). M: molecular weight marker; 1, 2: straw protein; 3, 4: husk protein.

**Table 4**
Inhibition capacity of DPPH and TEAC radicals of the protein concentrates extracted at a concentration of 10 mg/ml.

| Source | DPPH Inhibition (%) | TEAC (μM/100g) |
|---|---|---|
| **Straw** | 25.599 ± 0.64 | 263.00 ± 0.00 |
| **Husk** | 25.327 ± 0.44 | 263.23 ± 0.00 |

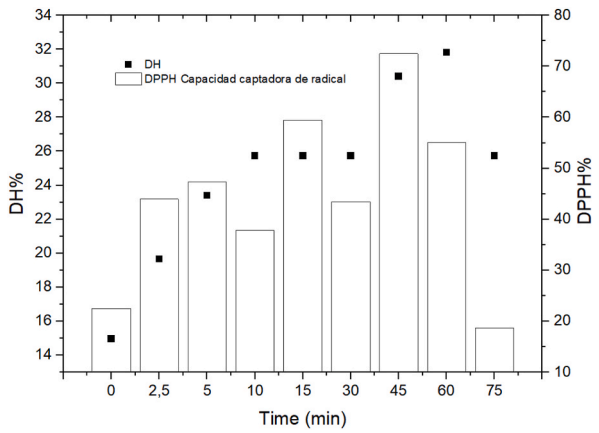


**Fig. 11.** Optimization of the hydrolysis process of protein extracts. Zero time is the process without adding enzyme, taken as hydrolysis control.

*3.6.1. Analysis of antioxidant capacity of protein hydrolysates*

It can also be seen a positive correlation between the degree of hydrolysis (DH) and the percentage of inhibition of the DPPH radical (Fig. 11), but there was not a total relationship with the hydrolysis time since there was no dependence between size and uptake of free radicals. The DPPH showed the best performance at 45 min compared to zero time, where an average inhibition percentage of 72.48% was obtained for the hydrolyzed protein compared to 22.47% for the non-hydrolyzed protein under the same test conditions, which stood for an increase of 322%.

These results set up the best hydrolysis conditions for both protein extracts using Alcalase® for 45 min, with an enzyme-substrate ratio of 1:10 and protein extract concentration of 20 mg/mL.

Enzymatic fragmentation to obtain hydrolysates of proteins of natural origin with antioxidant properties, with different types of

enzymes, has been widely reported previously using rice bran as a source [98–100]. The above data open the possibility of exploring these rice wastes for application in cosmetics, since currently cosmetics industries are intensely searching for ingredients with different bioactivities, one of the most relevant being those that help control or improve the signs of the aging process: **the antioxidant activity**, typical of many natural substances, which, applied at the dermal level, can help fight free radicals and are used for skin care products with antiaging claims.

The first electrophoretic band of both protein concentrates disappeared significantly as the hydrolysis time elapsed (Fig. 12), obtaining polypeptides with characteristic bands between approximately 60 and 75 kDa and a faint band close to 50 kDa. However, as for the unhydrolyzed proteins, the electrophoretic pattern is very similar for the hydrolysates of the two sources of residues used; the procedure and the amount seeded was the same in all wells, including the unhydrolyzed protein, for which when observing the size of the band in well 1 shows a reduction of the original band in the 6 wells corresponding to the hydrolysis, which also suggests the obtaining of at least two polypeptides, which is consistent with GH.

The protein hydrolysates obtained in the present research can become a profitable and sustainable alternative for the use of peptides and protein derivatives in cosmetics with antioxidant activity, but it is necessary to carry out additional studies such as skin permeability, dermal irritation tests and studies of effectiveness that support the anti-aging claim that has been presented in this study.

The scope of the article did not contemplate obtaining samples for direct application of cellulose, silicates or protein hydrolysates, but rather precursors with potential activity in the cosmetic field, because these precursors require more refinement and purification to match commercially available products, which is why they were not evaluated against these standards such as different types of cellulose, silicates or protein derivatives, which are used in cosmetic products. However, some references are provided, that support the potential properties of the rice husk and straw substrates that support the previously reported obtaining and their application in the cosmetic industry, as is the case of the use of cellulose [101], silicates [102] and hydrolyzed proteins [103].

## 4. Conclusion

The pollution stemming from waste generated by the agroindustry can be significantly reduced and, instead, turned into a source of added value. There is a global trend towards replacing chemically synthesized components with natural ingredients, especially in the cosmetics industry. This aligns with the increasing emphasis on personal care, anti-aging solutions, and a population that increasingly prefers natural cosmetic products while demonstrating greater environmental responsibility.

The results of our study, which focused on straw and husk derived from rice cultivation, revealed a high concentration of polysaccharides, an average level of ash content, and a low percentage of proteins. The characterization of bioactive substances obtained from these extracted macromolecules was aimed at harnessing their potential as high-value inputs. This can be achieved at a low cost and with substantial impact, thanks to the growing demand for natural ingredients in the development of cosmetic formulations. Additionally, the preliminary properties suggested that these substances can either be used directly or modified to enhance their performance.

## Ethical statement

Ethical approval and patient consent to participate are not applicable to this study because there were no patients involved in the study.

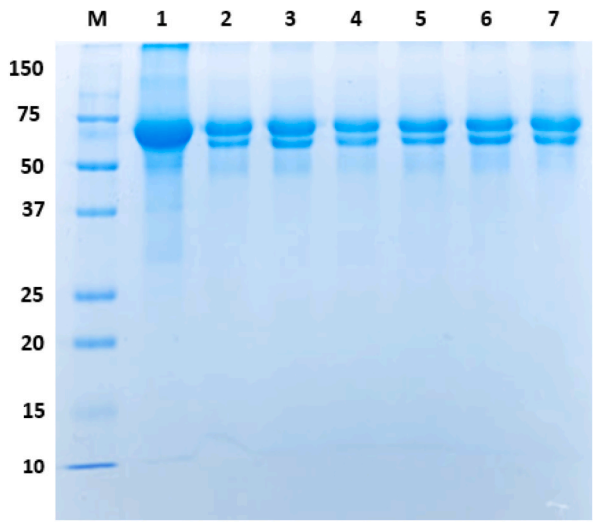


**Fig. 12.** Electrophoretic pattern (SDS-PAGE) of the hydrolyzed proteins. M, Molecular weight marker; 1, non-hydrolyzed straw protein; 2, 3 and 4, PPH (hydrolyzed straw protein); 5, 6 and 7, PCH (hydrolyzed husk protein).

## Data availability statement

The data associated with our work has not been deposited into a public repository. The data will be available on request.

## CRediT authorship contribution statement

**Paola Vargas-Escobar:** Writing – original draft, Investigation, Conceptualization. **Oscar Flórez-Acosta:** Writing – review & editing, Project administration, Funding acquisition, Formal analysis, Data curation, Conceptualization. **Ligia Luz Corrales-García:** Writing – review & editing, Methodology.

## Declaration of competing interest

The authors declare that they have no known competing financial interests or personal relationships that could have appeared to influence the work reported in this paper.

## Acknowledgments

The authors present a special acknowledgement to the 2017 programmatic announcement of the Committee for the Development of Research (CODI), of the University of Antioquia, for the financial support of this research.

## References

[1] FAO, Perspectivas de cosechas y situación alimentaria. Informe trimestral mundial N.o 4, diciembre 2022, Páginas 11-12 (2023). https://doi.org/10.4060/cc3233es.
[2] Rice Knowledge Bank, Rice by products [Internet] [cited 2019 May 2]. Available from: http://www.knowledgebank.irri.org/step-by-step-production/postharvest/rice-by-products#rice-bran, 2019.
[3] L. Truong, D. Morash, Y. Liu, A. King, Food waste in animal feed with a focus on use for broilers, Int J Recycl Org Waste Agric [Internet] 8 (4) (2019) 417–429, https://doi.org/10.1007/s40093-019-0276-4.
[4] T. Fujiwaki, K. Furusho, The effects of rice bran Broth bathing in patients with Atopic Dermatitis, Pediatr. Int. 34 (5) (1992) 505–510.
[5] D. Abril, E.A. Navarro, A.J. Abril, La paja de arroz, consecuencias de su manejo y alternativas de aprovechamiento, Rev la Fac Agron 17 (January) (2009) 69–79.
[6] J. Rojas, A. Lopez, S. Guisao, C. Ortiz, Evaluation of several microcrystalline celluloses obtained from agricultural by-products, J Adv Pharm Technol Res 2 (3) (2011) 144.
[7] J.K. Saini, R. Saini, L. Tewari, Lignocellulosic agriculture wastes as biomass feedstocks for second-generation bioethanol production: concepts and recent developments, 3 Biotech [Internet] 5 (4) (2015) 337–353, https://doi.org/10.1007/s13205-014-0246-5.
[8] R. Schramm, Value-added Processing of Rice and Rice By-Products [Internet], Louisiana State University, 2010. Available from: http://etd.lsu.edu/docs/available/etd-04092010-162834/.
[9] A.A. Sundarraj, T.V. Ranganathan, A review on cellulose and its utilization from agro-industrial waste, Drug Invent Today [Internet] 10 (1) (2018) 89–94. Available from: https://www.scopus.com/inward/record.uri?eid=2-s2.0-85045511581&partnerID=40&md5=b316ae7e3e7101d483e55f8bb56f7e3b.
[10] H. Ullah, H.A. Santos, T. Khan, Applications of bacterial cellulose in food, cosmetics and drug delivery, Cellulose 23 (4) (2016) 2291–2314.
[11] C.G. Ramos, J.C. Hower, E. Blanco, M.L.S. Oliveira, S.H. Theodoro, Possibilities of using silicate rock powder: an overview, Geosci Front [Internet] 13 (1) (2022) 101185, https://doi.org/10.1016/j.gsf.2021.101185.
[12] G. Gadikota, K. Fricker, S.H. Jang, A.H.A. Park, Carbonation of Silicate Minerals and Industrial Wastes and Their Potential Use as Sustainable Construction Materials, 2015, pp. 295–322.
[13] K. Kaviyarasu, E. Manikandan, J. Kennedy, M. Jayachandran, M. Maaza, Rice husks as a sustainable source of high quality nanostructured silica for high performance Li-ion battery requital by sol-gel method - a review, Adv. Mater. Lett. 7 (9) (2016) 684–696.
[14] R. Sekifuji, L Van Chieu, M. Tateda, H. Takimoto, Solubility and physical composition of rice husk ash silica as a function of calcination temperature and duration, Int. J. Recycl. Org. Waste Agric. 10 (1) (2021) 19–27.
[15] M. Deng, G. Zhang, X. Peng, J. Lin, X. Pei, R. Huang, A facile procedure for the synthesis of δ-Na2Si2O5 using rice husk ash as silicon source, Mater Lett [Internet] 163 (2016) 36–38, https://doi.org/10.1016/j.matlet.2015.10.046.
[16] S.A. Greenberg, The nature of the silicate species in sodium silicate solutions, J. Am. Chem. Soc. 80 (24) (1958) 6508–6511.
[17] F.A. Andersen, Final report on the safety assessment of potassium silicate, sodium metasilicate, and sodium silicate, Int. J. Toxicol. 24 (SUPPL. 1) (2005) 103–117.
[18] F. Wu, J. Deng, L. Hu, Z. Zhang, H. Jiang, Y. Li, et al., Investigation of the stability in Pickering emulsions preparation with commercial cosmetic ingredients, Colloids Surfaces A Physicochem Eng Asp [Internet] 602 (March) (2020) 125082, https://doi.org/10.1016/j.colsurfa.2020.125082.
[19] K. Fields, T.J. Falla, K. Rodan, L. Bush, Bioactive peptides: Signaling the future, J. Cosmet. Dermatol. 8 (1) (2009) 8–13.
[20] M.S. Ferreira, I.F. Almeida, M.C. Magalhães, J.M. Sousa-Lobo, Trending anti-aging peptides, Cosmetics 7 (4) (2020) 1–15.
[21] K. Lintner, Peptides and proteins, in: Z.D. Draelos (Ed.), Cosmetic Dermatology: Products and Procedures, third ed., 2022 [Internet], https://onlinelibrary.wiley.com/doi/chapter-epub/10.1002/9781119676881.ch38.
[22] Godi Aleksandar, Poljšak Borut, Adamic Metka, D. Raja, The role of antioxidants in cancer prevention and treatment, Indoor Built Environ. 12 (6) (2003) 401–404.
[23] M.S. Matsui, A. Hsia, J.D. Miller, K. Hanneman, H. Scull, K.D. Cooper, et al., Non-sunscreen photoprotection: antioxidants add value to a sunscreen, J Investig Dermatology Symp Proc [Internet] 14 (1) (2009) 56–59, https://doi.org/10.1038/jidsymp.2009.14.
[24] L. Liu, D.L.E. Waters, T.J. Rose, J. Bao, G.J. King, Phospholipids in rice: significance in grain quality and health benefits: a review, Food Chem [Internet] 139 (1–4) (2013) 1133–1145, https://doi.org/10.1016/j.foodchem.2012.12.046.
[25] Y. Shinji, S. Michiru, N. Ephantus, K. Mikio, M. Teruo, Protective mechanism of rice-derived lipids and Glucosylceramide in an in vitro Intestinal Tract model, J Agric Food Chem [Internet] (2016) 1–23. https://pubs.acs.org/doi/10.1021/acs.jafc.1c04562.
[26] T.G. Korotkova, S.J. Ksandopulo, A.P. Donenko, S.A. Bushumov, A.S. Danilchenko, Physical properties and chemical composition of the rice husk and dust, Orient. J. Chem. 32 (6) (2016) 3213–3219.
[27] Association of Official Analytical Chemist (AOAC), Volume II, in: Official Methods of Analysis, 2000.
[28] O.M.S. Cereales, legumbres, leguminosas y productos vegetales, in: Codex Alimentarius, Roma, 2007.
[29] A.A. Albalasmeh, A.A. Berhe, T.A. Ghezzehei, A new method for rapid determination of carbohydrate and total carbon concentrations using UV spectrophotometry, Carbohydr. Polym. 97 (2) (2013) 253–261, https://doi.org/10.1016/j.carbpol.2013.04.072 [Internet].

[30] Z. Dische, E. Borenfreud, A new spectrophotometric method for the detection and determination of keto sugars and trioses, J Biol Chem [Internet] 192 (2) (1951) 583–587, https://doi.org/10.1016/S0021-9258(19)77782-5.
[31] M. Valdez, D. Oziel, B. Gama, G. Muñoz, S. Sergio, O. Cerrilla, et al., Disponible en. http://www.redalyc.org/articulo.oa?id=43717102, 2006.
[32] J.M. Walker, The bicinchoninic acid (BCA) assay for protein quantitation, Methods Mol. Biol. 32 (1994) 5–8.
[33] L. Ye, W. Zhengxuan, L. Hui, L. Mingcai, Y. Lin, In vitro antioxidant activity of rice protein affected by alkaline degree and gastrointestinal protease digestion, J. Sci. Food Agric. (1) (2013) 51–58.
[34] Merck, Universal Protease Activity Assay Using Casein as a Substrate [Internet], 2020. https://www.sigmaaldrich.com/CO/es/technical-documents/protocol/protein-biology/elisa/protease-activity-assay.
[35] Ghribi A. Mokni, I. Maklouf Gafsi, A. Sila, C. Blecker, S. Danthine, H. Attia, et al., Effects of enzymatic hydrolysis on conformational and functional properties of chickpea protein isolate, Food Chem [Internet] 187 (2015) 322–330, https://doi.org/10.1016/j.foodchem.2015.04.109.
[36] N. Mohd Esa, T.B. Ling, By-products of rice processing: an overview of health benefits and applications, Rice Res Open Access 4 (1) (2016) 1–11.
[37] D. Dhingra, M. Michael, H. Rajput, R.T. Patil, Dietary fibre in foods: a review, J. Food Sci. Technol. 49 (3) (2012) 255–266.
[38] B.C. Saha, M.A. Cotta, Lime pretreatment, enzymatic saccharification and fermentation of rice hulls to ethanol, Biomass Bioenergy 32 (10) (2008) 971–977.
[39] S. Gallegos Tintoré, L. Chel Guerrero, L.J. Corzo Ríos, A.L. Martínez Ayala, Péptidos con actividad antioxidante de proteínas vegetales, in: Bioactividad de péptidos derivados de proteínas alimentarias, 2013, pp. 111–122. OmniaScien.
[40] Vásquez A. Sánchez, Bioactive peptides: a review, Int J Bioautomation. 15 (4) (2011) 223–250.
[41] M. Ferri, J. Graen-Heedfeld, K. Bretz, F. Guillon, E. Michelini, M.M. Calabretta, et al., Peptide fractions obtained from rice by-products by means of an environment-friendly process show in vitro health-related bioactivities, PLoS One 12 (1) (2017) 1–14.
[42] S. Gallegos-Tintoré, C. Torres-Fuentes, A.L. Martínez-Ayala, J. Solorza-Feria, M. Alaiz, J. Girón-Calle, et al., Antioxidant and chelating activity of Jatropha curcas L. protein hydrolysates, J. Sci. Food Agric. 91 (9) (2011) 1618–1624.
[43] A. Pihlanto, Antioxidative peptides derived from milk proteins, Int. Dairy J. 16 (11) (2006) 1306–1314.
[44] S. Banerjee, R. Sen, R.A. Pandey, T. Chakrabarti, D. Satpute, B.S. Giri, et al., Evaluation of wet air oxidation as a pretreatment strategy for bioethanol production from rice husk and process optimization, Biomass and Bioenergy [Internet] 33 (12) (2009) 1680–1686, https://doi.org/10.1016/j.biombioe.2009.09.001.
[45] A.K. K Kasymalieva, Pectins of Tobacco stems, rice strae and Kenaf Chaff 1 (1991) 2–5 [Internet], http://thesis.ekt.gr/thesisBookReader/id/1834#page/104/mode/2up.
[46] J.Y. Park, T. Seyama, R. Shiroma, M. Ike, S. Srichuwong, K. Nagata, et al., Efficient recovery of glucose and fructose via enzymatic saccharification of rice straw with soft carbohydrates, Biosci. Biotechnol. Biochem. 73 (5) (2009) 1072–1077.
[47] L.C. Yeng, M.U. Wahit, N. Othman, Thermal and flexural properties of regenerated CELLULOSE(RC)/POLY(3- HYDROXYBUTYRATE)(PHB)biocomposites lee, J Teknol Full 1 (2015) 1–6.
[48] D.F. Arseneau, Competitive reactions in the thermal decomposition of cellulose, Can. J. Chem. 49 (4) (1971) 632–638.
[49] H.S. Barud, A.M.D.A. Júnior, RMN De Assunção, C.S. Meireles, A. Daniel, Thermal characterization of cellulose acetate produced from homogeneous, Thermochim. Acta 471 (1) (2008) 61–69 [Internet], http://dc.engconfintl.org/biorefinery_I/.
[50] C.F. Liu, R.C. Sun, Cellulose [Internet]. 1st Ed. Cereal Straw as a Resource for Sustainable Biomaterials and Biofuels, Elsevier, 2010, pp. 131–167, https://doi.org/10.1016/B978-0-444-53234-3.00005-5.
[51] N. Johar, I. Ahmad, A. Dufresne, Extraction, preparation and characterization of cellulose fibres and nanocrystals from rice husk, Ind Crops Prod [Internet] 37 (1) (2012) 93–99, https://doi.org/10.1016/j.indcrop.2011.12.016.
[52] P. Kahar, Synergistic effects of pretreatment process on enzymatic digestion of rice straw for efficient ethanol fermentation, in: Environmental Biotechnology - New Approaches and Prospective Applications, 2013.
[53] D. Klemm, B. Heublein, H.P. Fink, A. Bohn, Cellulose: fascinating biopolymer and sustainable raw material, Angew. Chem. Int. Ed. 44 (22) (2005) 3358–3393.
[54] R. Singh, S. Tiwari, M. Srivastava, A. Shukla, Experimental study on the performance of microwave assisted hydrogen peroxide (H2O2) pretreatment of rice straw, Agric. Eng. Int. CIGR J. 16 (1) (2014) 173–181.
[55] A.D. French, M. Santiago Cintrón, Cellulose polymorphy, crystallite size, and the segal crystallinity index, Cellulose 20 (1) (2013) 583–588.
[56] S. Morales De La Rosa, HIDRÓLISIS ÁCIDA DE CELULOSA Y BIOMASA LIGNOCELULÓSICA ASISTIDA CON LÍQUIDOS IÓNICOS MEMORIA Para aspirar al grado de, vol. 15, 2015.
[57] G. Lamberti, G.W.M. Peters, G. Titomanlio, Crystallinity and linear rheological properties of polymers, Int. Polym. Process. 22 (3) (2007) 303–310.
[58] A.L. Jhon Rojas, Producción de un excipiente celulósico multipropósito, 2013.
[59] Susann Wiechers, J.M. Frank Unger, Use of Powdered Cellulose in Cosmetic Applications, 2013.
[60] J. Turrado, A.R. Saucedo, J. Ramos, M.L. Reynoso, Comportamiento de la fibra de celulosa reciclada en el proceso de hidratación, Inf. Tecnol. 19 (5) (2008) 129–136.
[61] S. Munshi, R.P. Sharma, Investigation on the pozzolanic properties of rice straw ash prepared at different temperatures, Mater Express 8 (2) (2018) 157–164.
[62] M.K. Naskar, D. Kundu, M. Chatterjee, Coral-like hydroxy sodalite particles from rice husk ash as silica source, Mater Lett [Internet] 65 (23–24) (2011) 3408–3410, https://doi.org/10.1016/j.matlet.2011.07.084.
[63] A.B.D. Nandiyanto, T. Rahman, M.A. Fadhlulloh, A.G. Abdullah, I. Hamidah, B. Mulyanti, Synthesis of silica particles from rice straw waste using a simple extraction method, IOP Conf. Ser. Mater. Sci. Eng. 128 (1) (2016).
[64] M.A. El-Sayed, T.M. El-Samni, Physical and chemical properties of rice straw ash and its effect on the cement paste produced from different cement types, J King Saud Univ - Eng Sci [Internet] 19 (1) (2006) 21–29, https://doi.org/10.1016/S1018-3639(18)30845-6.
[65] H. Moayedi, B. Aghel, M.M. Abdullahi, H. Nguyen, A. Safuan, A. Rashid, Applications of rice husk ash as green and sustainable biomass, J Clean Prod [Internet] 237 (2019) 117851, https://doi.org/10.1016/j.jclepro.2019.117851.
[66] J. Roselló, L. Soriano, M.P. Santamarina, J.L. Akasaki, J. Monzó, J. Payá, Rice straw ashA potential pozzolanic supplementary material for cementing systems, Ind Crops Prod [Internet] 103 (2017) 39–50, https://doi.org/10.1016/j.indcrop.2017.03.030.
[67] A. Miller, W. Charles, Nfrared spectra and characteristic frequencies of inorganic ions, Wuli Xuebao/Acta Physica Sinica. 24 (1954) 1253–1294.
[68] X. Ying-Mei, Q. Ji, H. De-Min, W. Dong-Mei, C. Hui-Ying, G. Jun, et al., Preparation of amorphous silica from oil shale residue and surface modification by silane coupling agent, Oil Shale 27 (1) (2010) 37–46.
[69] N.C.S. Selvam, R.T. Kumar, L.J. Kennedy, J.J. Vijaya, Comparative study of microwave and conventional methods for the preparation and optical properties of novel MgO-micro and nano-structures, J Alloys Compd [Internet] 509 (41) (2011) 9809–9815, https://doi.org/10.1016/j.jallcom.2011.08.032.
[70] H. Hamdan, M.N.M. Muhid, S. Endud, E. Listiorini, Z. Ramli, Si MAS NMR, XRD and FESEM studies of rice husk silica for the synthesis of zeolites, J. Non-Cryst. Solids 211 (1–2) (1997) 126–131.
[71] I. Tsuyumoto, High flame retardancy of amorphous sodium silicate on poly(ethylene-co-vinyl acetate) (EVA), Polym Bull [Internet] 75 (11) (2018) 4967–4976, https://doi.org/10.1007/s00289-018-2311-4.
[72] X. Hao, X. Hu, Z. Luo, T. Liu, Z. Li, T. Wu, et al., Preparation and properties of transparent cordierite-based glass-ceramics with high crystallinity, Ceram Int [Internet] 41 (10) (2015) 14130–14136, https://doi.org/10.1016/j.ceramint.2015.07.034.
[73] A. Trubetskaya, P.A. Jensen, A.D. Jensen, M. Steibel, H. Spliethoff, P. Glarborg, et al., Comparison of high temperature chars of wheat straw and rice husk with respect to chemistry, morphology and reactivity, Biomass and Bioenergy [Internet] 86 (2016) 76–87, https://doi.org/10.1016/j.biombioe.2016.01.017.
[74] S.R. Teixeira, R.S. Magalhães, A. Arenales, A.E. Souza, M. Romero, J.M. Rincón, Valorization of sugarcane bagasse ash: producing glass-ceramic materials, J Environ Manage [Internet] 134 (2014) 15–19, https://doi.org/10.1016/j.jenvman.2013.12.029.
[75] Y. Tang, W. Chen, Effect of Magnesium on the Structure and Chemical Composition of Calcium Silicate Hydrate at Elevated Temperature, vol. 240, Constr Build Mater [Internet], 2020 117925, https://doi.org/10.1016/j.conbuildmat.2019.117925.

[76] Z. Li, T. Zhang, J. Hu, Y. Tang, Y. Niu, J. Wei, et al., Characterization of reaction products and reaction process of MgO-SiO 2-H2O system at room temperature, Construct. Build. Mater. 61 (2014) 252–259.
[77] F. Jin, K. Gu, A. Al-Tabbaa, Strength and hydration properties of reactive MgO-activated ground granulated blastfurnace slag paste, Cem Concr Compos [Internet] 57 (2015) 8–16, https://doi.org/10.1016/j.cemconcomp.2014.10.007.
[78] D. Bhat Panemangalore, R. Shabadi, D. Tingaud, M. Touzin, G. Ji, Biocompatible silica-based magnesium composites, J. Alloys Compd. 772 (2019) 49–57, https://doi.org/10.1016/j.jallcom.2018.09.060 [Internet].
[79] F. Cheng, Y. Hu, Q. Song, J. Nie, J. Su, Y. Chen, Effect of curing temperature on the properties of a MgO-SiO2-H2O system prepared using dead-burned MgO, Materials 15 (17) (2022).
[80] Z. Li, Y. Xu, H. Liu, J. Zhang, J. Wei, Q. Yu, Effect of the MgO/silica fume ratio on the reaction process of the MgO-SiO2-H2O system, Materials 12 (1) (2018) 1–12.
[81] J. Zhou, Y. Su, J. Zhang, X. Xu, J. Zhao, G. Qian, et al., Distribution of OH bond to metal-oxide in Mg3-xCaxFe-layered double hydroxide (x=0-1.5): its role in adsorption of selenate and chromate, Chem Eng J [Internet] 262 (2015) 383–389, https://doi.org/10.1016/j.cej.2014.10.010.
[82] T.K. Ivanova, I.P. Kremenetskaya, V.V. Marchevskaya, M.V. Slukovskaya, S.V. Drogobuzhskaya, Magnesium silicate binding materials formed from heat-treated serpentine-group minerals and aqueous solutions: structural features. Acid-Neutralizing Capacity, and Strength Properties, Press Vessel Pip Technol, 2022.
[83] L. Xu, Y. Hu, Y. Mu, F. Zhang, J. Wang, W. Chen, et al., Kinetics of foaming process of potassium silicate gel at high temperature, Mater Lett [Internet] 281 (2020) 128614, https://doi.org/10.1016/j.matlet.2020.128614.
[84] Y. Li, F. Lu, C. Luo, Z. Chen, J. Mao, C. Shoemaker, et al., Functional properties of the Maillard reaction products of rice protein with sugar, Food Chem [Internet] 117 (1) (2009) 69–74, https://doi.org/10.1016/j.foodchem.2009.03.078.
[85] Suquilanda M tatiana Naranjo, Obtención de concentrado proteico por hidrólisis enzimática a partir del salvado de arroz de variedades ecuatorianas. Escuela superior politécnica del litoral, 2013 [Internet], http://www.dspace.espol.edu.ec/xmlui/handle/123456789/30919.
[86] F.A.S. Dairo, S.W. Ogunlade, T.A. Oluwasola, Proximate composition and amino acid profile of rice husk biodegraded with Pleurotus ostreatus for different periods. African J Food, Agric Nutr Dev 17 (3) (2017) 12243–12255.
[87] H.Y. Park, J. Sung, B.S. Kim, S.K. Ha, Y. Kim, Effect of degree of rice milling on antioxidant components and capacities, Ital. J. Food Sci. 30 (1) (2018) 50–60.
[88] L. Wattanasiritham, S. Kubglomsong, C. Theerakulkait, Antioxidant activity of rice bran protein extract, its enzymatic hydrolysates and its combination with commercial antioxidants, Pakistan J. Nutr. 14 (10) (2015) 647–652.
[89] A.A. Zaky, Z. Chen, M. Qin, M. Wang, Y. Jia, Assessment of antioxidant activity, amino acids, phenolic acids and functional attributes in defatted rice bran and rice bran protein concentrate, Prog. Nutr. 22 (4) (2020).
[90] A.A. Elzaawely, H.F. Maswada, M.E.A. El-Sayed, M.E. Ahmed, Phenolic compounds and antioxidant activity of rice straw extract, Int. Lett. Nat. Sci. 64 (July) (2017) 1–9.
[91] S. De, S. Mishra, E. Poonguzhali, M. Rajesh, K. Tamilarasan, Fractionation and characterization of lignin from waste rice straw: biomass surface chemical composition analysis, Int J Biol Macromol [Internet] 145 (2020) 795–803, https://doi.org/10.1016/j.ijbiomac.2019.10.068.
[92] T.N. Minh, T.D. Xuan, A. Ahmad, A.A. Elzaawely, R. Teschke, T.M. Van, Efficacy from different extractions for chemical profile and biological activities of rice husk, Sustain. Times 10 (5) (2018) 1–15.
[93] E. Karimi, P. Mehrabanjoubani, M. Keshavarzian, E. Oskoueian, H.Z. Jaafar, A. Abdolzadeh, Identification and quantification of phenolic and flavonoid components in straw and seed husk of some rice varieties (Oryza sativa L.) and their antioxidant properties, J. Sci. Food Agric. 94 (11) (2014) 2324–2330.
[94] A.A. Intiquilla, Evaluación de la actividad antioxidante de las fracciones peptídicas de hidrolizados proteínicos obtenidos a partir de semillas de Erythrina edulis, UNIVERSIDAD NACIONAL MAYOR DE SAN MARCOS, 2015.
[95] L. Wattanasiritham, C. Theerakulkait, S. Wickramasekara, C.S. Maier, J.F. Stevens, Isolation and identification of antioxidant peptides from enzymatically hydrolyzed rice bran protein, Food Chem [Internet] 192 (2016) 156–162, https://doi.org/10.1016/j.foodchem.2015.06.057.
[96] A.P. Adebiyi, A.O. Adebiyi, J. Yamashita, T. Ogawa, K. Muramoto, Purification and characterization of antioxidative peptides derived from rice bran protein hydrolysates, Eur. Food Res. Technol. 228 (4) (2009) 553–563.
[97] X.Q. Zheng, L Te Li, X.L. Liu, X.J. Wang, J. Lin, D. Li, Production of hydrolysate with antioxidative activity by enzymatic hydrolysis of extruded corn gluten, Appl. Microbiol. Biotechnol. 73 (4) (2006) 763–770.
[98] V. Bregola, S. Bosi, S. Hrelia, E. Leoncini, G. Dinelli, M. Malaguti, et al., Bioactive peptides in cereals and legumes: agronomical, biochemical and clinical aspects, Int. J. Mol. Sci. 15 (11) (2014) 21120–21135.
[99] J.S. Hamada, Characterization and functional properties of rice bran proteins modified by commercial exoproteases and endoproteases, J. Food Sci. 65 (2) (2000) 305–310.
[100] M.A. Mazorra-Manzano, J.C. Ramírez-Suarez, R.Y. Yada, Plant proteases for bioactive peptides release: a review, Crit. Rev. Food Sci. Nutr. 58 (13) (2018) 2147–2163.
[101] Saumya Singh, Gurkanwal Kaur, Devendra P. Singh, Shailendra Kumar Arya, Meena Krishania, Exploring rice straw's potential from a sustainable biorefinery standpoint: Towards valorization and diverse product production, Process Safety and Environmental Protection, Volume 184, 2024, Pages 314-331, ISSN 0957-5820, https://doi.org/10.1016/j.psep.2024.01.105.https://www.sciencedirect.com/science/article/pii/S0957582024001204.
[102] Stella Emmanuel, Alhassan Sallau, Adedirin Ibrahim Oluwaseye, Buga Hussain, Okereke Mohammed, Ozonyia Anthony, Alabi F. Gertrude, Synthesis of sodium silicate crystals from rice husk ash, J Serbian Chem Soc 88 (2023) 40.
[103] R. Esfandi, M.E. Walters, A. Tsopmo, Antioxidant properties and potential mechanisms of hydrolyzed proteins and peptides from cereals, Heliyon 5 (4) (2019) e01538, https://doi.org/10.1016/j.heliyon.2019.e01538 [Internet].